Silver(I) and zinc(II) complexes with symmetrical cinnamaldehyde Schiff base derivative: Spectroscopic, powder diffraction characterization, and antimycobacterial studies

Thaeny C. Amaral [a], Fábio B. Miguel [b], Mara R.C. Couri [b], Pedro P. Corbi [c], Marcos A. Carvalho [c], Débora L. Campos [d], Fernando R. Pavan [d], Alexandre Cuin [a,*]

[a] LQBin, Laboratório de Química BioInorgânica, Departamento de Química, Instituto de Ciências Exatas, UFJF, 36330-330 Juiz de Fora, MG, Brazil
[b] Departamento de Química, Instituto de Ciências Exatas, UFJF, 36036-330 Juiz de Fora, MG, Brazil
[c] Instituto de Química, Universidade Estadual de Campinas, UNICAMP, 13083-970, Campinas, SP, Brazil
[d] Laboratório de Pesquisas em Tuberculose, Departamento de Ciências Biológicas, Faculdade de Ciências Farmacêuticas, UNESP, 14801-903 Araraquara, SP, Brazil

ABSTRACT

Silver(I) and zinc(II) complexes with *N,N'*-bis(*trans*-cinnamaldehyde)ethane-1,2-diamine (EnCinn) have been synthesized and characterized by elemental analysis, simultaneous thermogravimetric and differential thermal studies (TG-DTA), infrared (IR), ^{1}H and ^{13}C nuclear magnetic resonance (NMR) spectroscopic measurements and electrospray ionization quadrupole time-of-flight mass spectrometry (ESI-QTOF-MS). Crystal and molecular structure descriptions were performed based on powder X-ray diffraction data. The AgEnCinn complex has a polymeric structure where the ligand bridges between two Ag(I) ions, while the ZnEnCinn complex has a monomeric structure with EnCinn acting as chelating ligand. Antimycobacterial assays over *Mycobacterium tuberculosis* showed the activity of the Ag(I) complex with Minimum Inhibitory Concentration (MIC) value of 22.7 μmol L^{-1}, while the Zn(II) complex was shown to be inactive over the same experimental conditions.

1. Introduction

Tuberculosis (TB) is an endemic disease that affect millions of people in many countries. TB is a common infection in populations living in poverty conditions, without adequate sanitation and in close contact with infectious vectors. In 2016, more than 6.3 million new cases of TB were reported, while in 2015 the number of cases informed was of 6.1 million. Besides the number of infected people increases year after year, drug-resistant TB is also a continuing threat. In 2016, there were nearly 600.000 new cases with resistance to rifampicin (RRTB), the most effective first-line drug [1]. Therefore, much effort has been expended to find new classes of compounds able to defeat the *Mycobacterium tuberculosis* – the mycobacterium that causes tuberculosis.

In this sense, many research groups around the world have addressed their research on metal complexes with therapeutic activities over *M. tuberculosis*, especially silver(I) complexes, since some compounds of this class have demonstrated high anti-TB activity. In our recent papers, silver(I) complexes with alfa-hydroxy acids [2], amino acids [3], benzothiazoles [4], mercaptopurines [5] and Schiff bases [6,7] synthesized in our laboratories, have shown to be more effective against *M. tuberculosis* than silver sulfadiazine (SSD), a standard and widely commercial silver(I) complex used in the treatment of bacterial infections in burns and skin wounds. Besides biological properties of Ag(I) ions, Zn(II) ions are essential factors for many biological processes and their complexes are present in a broad spectrum of biological functions [8]. Indeed, our group has been looking for ligands from natural sources and with biological properties. In this way, Ag(I) and Zn(II) ions were combined with a *N*-donor ligand from cinnamaldehyde (CA), a major constituent of cinnamon essential oil, extracted from bark of cinnamon trees of the *Cinnamomum* genus. CA is also a natural antimicrobial substance that is generally recognized as safe (GRAS) by the U.S. Food and Drug Administration. Since cinnamaldehyde has conjugated double bonds with C=O group, it forms stable Schiff bases with amine compounds (–NH$_2$) [9].

In this paper we report the synthesis of new Ag(I) and Zn(II) complexes with the symmetrical Schiff base *N,N'*-bis(*trans*-cinnamaldehyde)ethane-1,2-diamine (EnCinn) and their structural characterizations based on spectroscopic and on powder X-ray

diffraction data. Biological studies of the complexes over *M. tuberculosis* are also reported.

2. Experimental

2.1. Materials and methods

Ethylenediamine (99%), *trans*-cinnamaldehyde (99%), silver nitrate (99%) and anhydrous zinc chloride (98%) were purchased from Sigma–Aldrich Laboratories. Elemental analyses of carbon, hydrogen and nitrogen were performed using a CHNS/O Perkin Elmer 2400 Analyzer. Infrared spectra were measured using a Spectrum 2000 FT-IR Perkin Elmer spectrophotometer in the range $4000–400 \, cm^{-1}$ with resolution of $4 \, cm^{-1}$; samples were prepared as KBr pellets.

The ^1H and ^{13}C NMR spectra of EnCinn were recorded on a Bruker Avance 500 MHz spectrophotometer, operating at 499.9 MHz for ^1H and at 125.7 MHz for ^{13}C. The ^1H and ^{13}C NMR spectra of AgEnCinn were recorded on a Bruker Avance 400 MHz spectrophotometer, operating at 400.1 MHz for ^1H and at 100.6 MHz for ^{13}C, while the ^1H and ^{13}C NMR spectra of ZnEnCinn were recorded on a Bruker Avance 600 MHz spectrophotometer, operating at 600.1 MHz for ^1H and at 150.9 MHz for ^{13}C; samples were prepared in deuterated dimethyl sulfoxide (DMSO). An additional study on the stability of the Ag(I) complex in DMSO by ^1H NMR spectroscopy was performed. In this case, a sample of the compound was prepared and immediately analyzed (time zero). Successive measurements of this sample were performed after 1, 2, 3, 6 and 24 h. The experiment was carried out in a Bruker Avance 400 MHz operating at 400.1 MHz for ^1H. Electrospray ionization quadrupole time-of-flight mass spectrometric measurements (ESI-QTOF-MS) were carried out in a Waters Xevo instrument. A sample of AgEnCinn complex was solubilized in methanol (0.1% formic acid v/v) at a concentration of 1 mg/mL, and then further diluted 100-fold in the same solvent mixture and immediately analyzed. Resulting solutions were directly infused into the instrument ESI source at a flow rate of $30 \, \mu L \, min^{-1}$. Typical acquisition conditions were capillary voltage 3 kV, sampling cone voltage 30 V and source temperature of 120 °C. Thermogravimetric and differential thermal analyses (TGA/DTA) were performed on a Simultaneous TGA/DTA SEIKO EXSTAR 6000 thermoanalyzer, using the following conditions: synthetic air, flow rate of $100 \, cm^3 \, min^{-1}$ and heating rate of $5 \, °C \, min^{-1}$ from 25 °C to 900 °C.

2.2. Synthesis of EnCinn and its Ag(I) and Zn(II) complexes

N,N′-bis(*trans*-cinnamaldehyde)ethane-1,2-diamine (EnCinn) was prepared following literature procedures [10]. Catena-{(μ-nitro-κ²O,O-)μ-bis(*trans*-cinnamaldehyde)ethane-1,2-diamine-κ²-*N,N′*]silver(I)} complex, hereafter represented as AgEnCinn, was obtained by adding 1.0 mmol (0.1700 g) of $AgNO_3$ dissolved in 10 mL of acetonitrile to 1.0 mmol (0.288 g) of EnCinn also dissolved in 30 mL of acetonitrile. The reaction was kept under

moderate heating (50 °C) for 1 h. A white polycrystalline solid was formed and collected by filtration, washed with acetonitrile and dried in a desiccator under silica. Following a similar procedure, {[*N,N′*-bis(*trans*-cinnamaldehyde)ethane-1,2-diamine)-κ²*N,N′*]dichloridezinc(II)} complex, labeled as ZnEnCinn, was obtained. However, 1.0 mmol (0.136 g) of $ZnCl_2$ was used instead of $AgNO_3$. The yellow polycrystalline solid formed was also collected by filtration and dried in desiccator under silica. Both filtered solutions were left to stand protected from light at room temperature for few weeks, but no single crystals suitable for X-ray diffraction study were obtained. Thus, powder diffraction methods to retrieve their crystal and molecular structures (vide infra) were employed. Elemental analyses and ancillary analytical data for free EnCinn and for its Ag(I) and Zn(II) complexes are shown in Table 1.

2.3. X-ray powder diffraction data collection and structure determination

Crystal structures of the Ag(I) and Zn(II) complexes were obtained by *state-of-the-art* powder diffraction data measured on conventional laboratory equipment. To perform the powder diffraction analyses, polycrystalline samples of AgEnCinn and ZnEnCinn were gently grounded in an agate mortar and each powder was deposited in hollow of thin glass sample-holder plate, with nearly zero-background. The diffraction data were collected by overnight scans in the 2θ range of 3.7–105° for AgEnCinn and 6–105° for ZnEnCinn with steps of 0.02° using a *Bruker AXS D8 da Vinci* diffractometer, equipped with Ni-filtered and Cu Kα radiation ($\lambda = 1.5418 \, Å$), a Lynxeye linear position-sensitive detector and the following optics: primary beam Soller slits (2.94°), fixed divergence slit (0.3°) and receiving slit (7.68 and 8.92 mm, for silver and zinc complexes, respectively). The generator was set at 40 kV and 40 mA. Approximate unit cell parameters were determined using 20 first standard peaks, followed by indexing through the single-value decomposition approach [11] implemented in TOPAS [12]. The space groups *C2/c* and *P2₁/c* were chosen for AgEnCinn and ZnEnCinn, respectively, after careful systematic absence analysis and both cell parameters were refined using 3.7(6)–55 2th range by Pawley method [13]. In both cases, no higher symmetric system was suggested by PLATON [14]. The structure solution process for both cases was performed by the simulated annealing technique [15] also implemented in TOPAS. In addition, the EnCinn rigid body model based on single-crystal data [16] was built using Z-matrix formalism, with free rotations and translations as well torsion angles as described in Chart 1. It is worth note that there is no free rotation for N1=C2 and C3=C4 axes due the double bonds between these atoms.

Torsion angles, rotation and translation parameters of the ligand were used in simulated annealing step for both structures. In the specific case of AgEnCinn complex, translation and rotation values for nitrate ion (built also as Z-matrix) were left free as well translational parameters of Ag(I) ions. In the case of ZnEnCinn, a second rigid body – $ZnCl_2$ was idealized with free rotation and

Table 1
Analytical and complementary data for EnCinn ligand and its complexes.

Compound	Formula (MW, g mol⁻¹)	Yield (%)	MP (°C)	Analytical data (%)		
				C	H	N
EnCinn	$C_{20}H_{20}N_2$ [288.0]	90	108	(83.0)	(6.84)	(9.60)
				[83.3]	[6.99]	[9.71]
AgEnCinn	$C_{20}H_{20}N_3O_3Ag$ [457.9]	70	dec*	(52.4)	(4.55)	(9.09)
				[52.4]	[4.40]	[9.17]
ZnEnCinn	$C_{20}H_{20}Cl_2N_2Zn$ [424.4]	87	dec*	(56.9)	(4.81)	(6.57)
				[56.6]	[4.74]	[6.60]

* Decompose over 300 °C. Experimental data were provided in parentheses while calculated ones are in brackets.
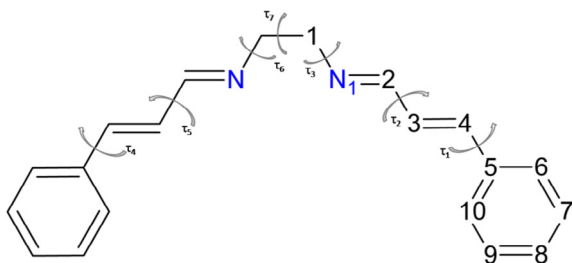
Chart 1. Sketch of EnCinn in *E*-isomer form where the torsion angles used in the simulated annealing and Rietveld refinement steps are described τ_1 to τ_7. Some of the carbon atoms were replaced by numbers and hydrogen atoms were omitted for a better visualization.

translation variables. However, Cl–Zn–Cl angle and Cl–Zn distance bonds were left free with soft constrains (angle within 100–120 degree and distance bonds 2.1–2.4 Å). In the refinement stage on AgEnCinn data, carried out by the Rietveld method [17], 38 parameters were refined including 6 parameters for background modeled by a Chebyshev polynomial function and a broad peak at 12.3° (2th) was inserted to describe the presence of a small amorphous portion. The rigid body description introduced at the solution stage was maintained in the final refinement. An isotropic thermal parameter set up at 3.0 (0.2) Å^2 was assigned to all atoms. For the ZnEnCinn case 39 parameters were refined, also using Rietveld method and, as usual, the 6 background parameters were modeled by a Chebyshev polynomial function.

2.4. Anti-M. tuberculosis activity assay

The *anti-M. tuberculosis* (anti-TB) activities of the compounds were determined by the Resazurin Microtiter Assay (REMA) method, as described in the literature [18]. Stock solutions of the tested compounds were prepared in DMSO at 10 g L^{-1} and diluted in Middlebrook 7H9 broth (Difco) supplemented with oleic acid, albumin, dextrose and catalase (OADC), performed by Precision XS (Biotek$^®$) to obtain the final drug concentration range of 0.09–25 µg mL^{-1}. Rifampicin was dissolved in dimethyl sufoxide and used as standard drugs. A suspension of the *M. tuberculosis* H$_{37}$Rv ATCC 27294 was cultured in Middlebrook 7H9 broth supplemented with OADC and 0.05% Tween 80. When the culture obtained a turbidity of McFarland standard No. 1, it was adjusted CFU by 5×10^5 CFU per mL and 100 µL of the inoculum were added to each well of a 96-well microplate together with 100 µL of the compounds. Samples were set up in three independent assays. The plates were incubated for 7 days at 37 °C. Resazurin (solubilized in water) was added (30 µL of 0.01%). The fluorescence of the wells was measured after 24 h with a Cytation 3 (Biotek$^®$). The Minimum Inhibitory Concentration (MIC) was defined as the lowest concentration resulting in 90% inhibition of growth of *M. tuberculosis*.

3. Results and discussion

3.1. Elemental analyses

Elemental analyses and complementary analytical data for EnCinn and its Zn(II) and Ag(I) complexes are shown in Table 1.

3.2. Spectroscopic studies

The infrared (IR) spectrum of EnCinn shows the characteristic bands of Schiff base compounds. The aromatic and aliphatic v (CH) stretchings are centered at 3070, 2924 and 2995 cm^{-1},

respectively. The $v(C=N)$ stretching frequency is observed at 1633 cm^{-1}, while bands at 1489 and 1448 cm^{-1} are assigned to v (C=C) frequencies [19].

The AgEnCinn and ZnEnCinn IR spectra are quite similar each other and they are also related to the IR spectrum of EnCinn. The spectra of compounds are supplied as Supplementary material – S1. The $v(C=N)$ was observed at 1633 cm^{-1} for the EnCinn ligand. The same vibrational mode is observed at 1630 cm^{-1} and 1636 cm^{-1} for the Ag(I) and Zn(II) complexes, respectively. It is worthy to note that, in similar structures, minor down/up shift in the v (C=N) band denotes the polymeric nature when ligand act as bridge, or 5 membered heterocycle rings when the ligand acts as a chelate [6]. In addition, for AgEnCinn, the strong band at 1384 cm^{-1} can be assigned to $v(NO)$ of the NO$_3^-$ group [6].

It was not possible to identify the M–L bands such as $v(ZnCl)$, v (ZnN), $v(AgN)$ and $v(AgO)$ since these bands fall at lower frequency than 400 cm^{-1} and they are overlapped from organic moiety frequencies.

The ^{1}H and ^{13}C NMR spectra of EnCinn and its Ag(I) and Zn(II) complexes show slight changes in the chemical displacement of the atoms near the coordination environment, thus confirming the formation of complexes as pointed out in Table 2.

To evaluate the stability of AgEnCinn complex in DMSO, additional ^{1}H NMR spectroscopic measurements with time were carried out. The compound has shown to be stable over 24 h. The NMR spectra obtained with time are presented as Supplementary material S2.

3.3. Mass spectrometric measurements

ESI(+)-QTOF-MS analysis of AgEnCinn (see Supplementary material S3) indicates the presence of [C$_{40}$H$_{40}$N$_4$Ag]$^+$ ions (m/z 685.220, C$_{40}$H$_{40}$N$_4$Ag$^+$) as the most abundant species, confirming the proposed composition for Ag(I) complex. The [C$_{20}$H$_{20}$N$_2$Ag]$^+$ ions were also observed with similar composition except for an additional loss of ligand (m/z 395.0587, C$_{20}$H$_{20}$N$_2$Ag$^+$). The experimental isotopic pattern for the most abundant [C$_{40}$H$_{40}$N$_4$Ag]$^+$ ion is in good agreement with the respective theoretical prediction (Fig. S2b). The mass error for this ion was −11.85 ppm (C$_{40}$H$_{40}$N$_4$-Ag$^+$, calcd. m/z 683.2304, exp. m/z 683.2173), considering the monoisotopic ion of the composition.

3.4. Thermal analysis

The thermogravimetric data confirmed the composition of the AgEnCinn complex formulated as C$_{20}$H$_{20}$AgN$_3$O$_3$. Oxidation of the

Table 2
Solution-state ^{1}H and ^{13}C{^{1}H} NMR data for EnCinn ligand and its complexes.

Carbon	Chemical Shifts (ppm)		
	EnCinn	AgEnCinn	ZnEnCinn
C1	61.3	61.6	58.9
C2	163.4	168.3	166.8
C3	127.2	127.4	126.2
C4	135.5	134.6	134.9
C5	141.3	145.5	144.9
C6, C10	128.8	128.8	129.0
C7,C9	129.1	130.0	129.9
C8	128.0	127.6	127.5
Hydrogen			
H–C1	3.71 s, 2H	4.00 s, 2H	3.81 s, 2H
H–C2	8.06 d, 1H	8.44 d, 1H	8.32 d, 1H
H–C3	6.91 m, 1H	7.08 m, 1H	7.07 m, 1H
H–C4	7.09 dd, 1H	7.26 dd, 1H	7.35 dd, 1H
H–C6, H–C10	7.57 dd, 2H	7.47 m, 2H	7.60 m, 2H
H–C7, H–C9 e H–C8	7.33 m, 3H	7.34 m, 3H	7.48 m, 3H

The carbon codes follow the labeling proposed in Chart 1.

ligand starts at 177 °C and continues until 543 °C, showing a mass loss of 77.2%. The residue of thermal decomposition matches with Ag^o (Calcd. 23.5%. Found 22.8%). In the DTA curve we can see exothermic peaks at 187 °C, 209 °C, 408 °C and 462 °C related to ligand oxidation. The TGA/DTA curves are presented as Supplementary material – S4.

3.5. Crystal structure studies

The crystal structures of the AgEnCinn and ZnEnCinn complexes were determined and refined by *state-of-art* powder diffraction data. As described in our papers previously published [20,21], the extensive uses of rigid body and over than 20 parameters in the simulated annealing stage does not allow a deep discussion of intramolecular features. Nevertheless, the analysis of the powder diffraction data combined with the spectroscopic and analytical results provided us robust crystal models. Indeed, important crystallochemical information such as stoichiometry, molecular con-

formation and connectivity, and overall crystal packing features could be afforded in both cases.

The sketch of the crystal model for silver complex is shown in Fig. 1 while the final Rietveld refinement plot is provided as Supplementary material S5. Table 3 contains the relevant crystal data for the silver and zinc complexes, while Table 4 contains selected bond distances and angles as well important interactions for the complexes.

In the AgEnCinn complex the bidentate ligand bridges between two Ag(I) centers avoiding chelation toward a single silver(I) ion like in similar silver complexes [6]. As expected, the Ag-N bridge induces the formation of an inorganic 1D polymer, growing up parallel to the *b* axis (see Fig. 2), where Ag–N and Ag–N′, bond distances are 2.399 Å and 2.298 Å, respectively. In addition, the nitrate group is also bonded to Ag(I) ions by only one oxygen atom at 2.30 Å. Furthermore, the same oxygen atom bonded to Ag(I) has a strong interaction with another Ag(I), by means of 2.957 Å. Since each Ag(I) is coordinated by two distinct ligands by their iminic
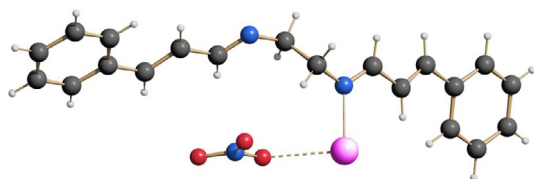

Fig. 1. The asymmetric unit of AgEnCinn complex. The silver(I) ion is colored in pink while carbon, hydrogen, nitrogen and oxygen atoms were colored as black, white, blue and red, respectively. (Color online.)

Table 3
Main crystallographic data of AgEnCinn and ZnEnCinn complexes.

	AgEnCinn	ZnEnCinn
Empirical formula	$C_{20}H_{20}AgN_3O_3$	$C_{20}H_{20}N_2Cl_2Zn$
Formula weight	457.87	424.29
T (K)	298	
λ (Cu Kα) (Å)	1.5418	
Crystal system	monoclinic	
Space group	$C2/c$	$P2_1/c$
a (Å)	40.850(1)	7.196(3)
b (Å)	11.636(3)	20.341(8)
c (Å)	8.554(2)	14.004(4)
β (°)	103.478(3)	94.961(2)
V (Å³)	3954.0(2)	2042.1(1)
Z	8	4
D_{calc} (g cm⁻³)	1.540	1.381
μ (mm⁻¹)	8.44	4.11
$F(000)$	1856	872
Number of parameters	38	39
R_{Bragg}, R_{wp}, GOF	0.024, 0.09, 8.3	0.057, 0.098, 10.9

Fig. 2. The 1D polymer of AgEnCinn parallel to *b* axis. All atoms were colored following code of Fig. 1. (Color online.)

Table 4
Selected distance and angle bonds and interactions of EnCinn complexes.

Complexes	Distance(Å)		Angle(°)	
AgEnCinn	Ag–N	2.399(2)	N–Ag–N′	166.12(1)
	Ag–N′	2.298(3)	N–Ag–O	98.13(2)
	Ag–O	2.330(2)	Ag–O--Ag″	110.17(5)
	Ag″--O	2.956(2)	N′–Ag–O	96.40(3)
ZnEnCinn			N–Zn–N	79.86(4)
	N1–Zn	2.171(1)	Cl–Zn–Cl	113.61(5)
	N21–Zn	2.228(1)	Cl1–Zn–N1	113.93(5)
	Cl1–Zn	2.142(9)	Cl1–Zn–N21	111.10(5)
	Cl2–Zn	2.126(9)	Cl2–Zn–N11	115.76(6)
			Cl2–Zn–N21	118.45(7)

Symmetry codes: i = 0.5 − *x*, 0.5 + *y*, 0.5 − *z*; ii = 0.5 − *x*, 1.5 − *y*, 1 − *z*. (−) bond and (--) interaction.
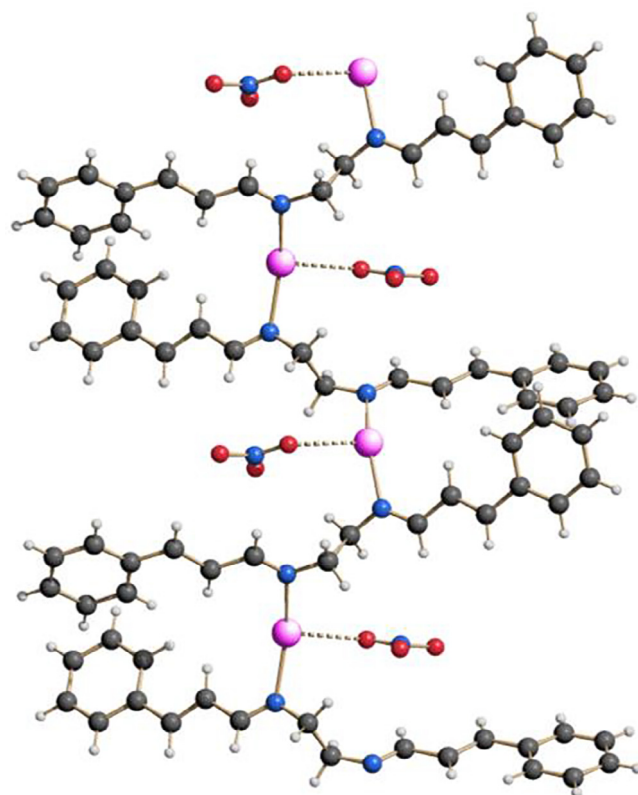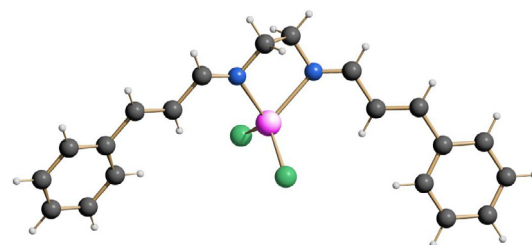

Fig. 3. The crystal structure model of ZnEnCinn. The pink sphere represents zinc(II), where it is surrounded by two chlorine ions (colored in green) and two nitrogen atoms (blue ones). The carbon and hydrogen atoms were represented in black and white colors, respectively. (Color online.)
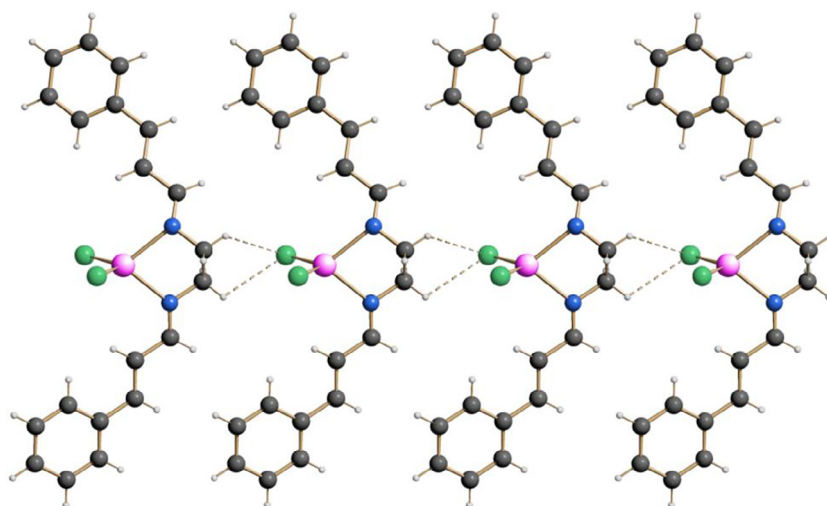
Fig. 4. The ZnEnCinn packing along *b* axis. The hydrogen atoms of the ethylene moiety interact with chlorine ions by about 2.93 Å. The color codes are the same used in Fig. 3. (Color online.)

Table 5
Biological results – anti-TB values for the free ligand, Ag(I) and Zn(II) complexes, SSD and the metal salts.

Compound	MW (g mol^{-1})	w%, Metal	MIC (mg L^{-1}) [µmol L^{-1}]
EnCinn	260	–	>25
AgEnCinn	457.9	23.5	10.4 [22.7]
ZnEnCinn	424.3	15.4	>25
SSD	357	30.2	7.80 [21.8]
Rifampicin	822.9	–	0.025 [0.03]
AgNO$_3$	169.9	63.5	12.5 [73.6]
ZnCl$_2$	136	48.0	>25

nitrogen atoms and by only one oxygen atom from the nitrate ion, and considering the bond distances and angles described in the Table 4, the Ag(I) coordination geometry can be described as a T-shaped geometry.

The crystal model for ZnEnCinn is shown in Fig. 3 and the final Rietveld refinement plot is provided as Supplementary material S6. The ZnEnCinn complex has a single molecular structure and the packing is generated by Cl⋯H–C weak interactions as shown in Fig. 4. The Zn(II) ion has the common *pseudo*-tetrahedral geometry, defined by two chlorides and one ligand, acting as chelating, as shown in Fig. 3 [22]. Indeed, the ethylenediamine moiety of the ligand makes a five-membered ring with angle N–Zn–N lower than 80°, as described in the Table 5.

3.6. Antituberculosis assay

Biological studies concerning the anti *M. tuberculosis* activity of EnCinn and the Ag(I) and Zn(II) complexes are shown in Table 5. In addition, the standard drug silver sulfadiazine (SSD) and the precursor salts AgNO$_3$ and ZnCl$_2$ were also evaluated against *M. tuberculosis* in the same experimental conditions. The values obtained are shown in Table 5.

As recently published [6], pure AgNO$_3$ solution is very toxic for *M. tuberculosis* as well for VERO cells suggesting that free silver ions should be avoided in biological systems. On the other hand, as described in Table 5, pure EnCinn does not possess biological activity against *M. tuberculosis*, indicating that the complexation of silver(I) with non-toxic organic molecules can afford new drugs with activity against TB. Hence, the AgEnCinn complex reported in

this work show activity against *M. tuberculosis* with MIC value of 22.7 µmol L^{-1} nearly to SSD reference (21.8 µmol L^{-1}). The ZnEnCinn complex showed no inhibitory activity against *M. tuberculosis* in the same experimental conditions.

4. Conclusion

Silver(I) and zinc(II) complexes with EnCinn were synthesized and presented molar compositions 1:1 metal/ligand. Chemical analyses confirmed the minimal formulas C$_{20}$H$_{20}$N$_2$AgNO$_3$ and C$_{20}$H$_{20}$N$_2$Cl$_2$Zn for the AgEnCinn and ZnEnCinn, respectively. Crystallographic studies were carried out using powder diffraction *state-of-art* technique. The AgEnCinn complex has a polymeric structure where EnCinn bridges between Ag(I) parallel to *b* axis. In the ZnEnCinn complex the ligand acts as a chelating agent and two independent chlorine ions complete the tetrahedral coordination around the Zn(II) center. The AgEnCinn showed good and promising biological activity against *M. tuberculosis*, showing MIC value of 10.4 mg L^{-1} or 22.7 µmol L^{-1}.

Appendix A. Supplementary data

CCDC 1538347 and 1538348 contains the supplementary crystallographic data. These data can be obtained free of charge via http://www.ccdc.cam.ac.uk/conts/retrieving.html, or from the Cambridge Crystallographic Data Centre, 12 Union Road, Cambridge CB2 1EZ, UK; fax: (+44) 1223-336-033; or e-mail: deposit@ccdc.cam.ac.uk. IR, ^{1}H NMR and mass spectra, along with Rietveld plots and TG/DTA curves for complexes and ligands, are available as supplementary materials. Supplementary data associated with this article can be found, in the online version, at https://doi.org/10.1016/j.poly.2018.02.024.

References

[1] Global Tuberculosis Report 2017. Geneva: World Health Organization 2017. ISBN 978-92-4-156551-6.

[2] A. Cuin, A.C. Massabni, C.Q.F. Leite, D.N. Sato, A. Neves, B. Szpoganicz, M.S. Silva, A.J. Bortoluzzi, Synthesis, X-ray structure and antimycobacterial Activity of Silver complexes with alfa-hydroxycarboxylic acids, J. Inorg. Biochem. 101 (2007) 291.

[3] G.A. Pereira, A.C. Massabni, E.E. Castellano, L.A. Sodré Costa, C.Q.F. Leite, F.R. Pavan, A. Cuin, A broad study of two new promising antimycobacterial drugs: Ag(I) and Au(I) complexes with 2-(2-thienyl)benzothiazole, Polyhedron 38 (2012) 291.

[4] G.S.M. Costa, P.P. Corbi, C. Abbehausen, A.L.B. Formiga, W.R. Lustri, A. Cuin, Silver(I) and gold(I) complexes with penicillamine: Synthesis, spectroscopic characterization and biological studies, Polyhedron 34 (2012) 210.

[5] A. Cuin, A.C. Massabni, G.A. Pereira, C.Q.F. Leite, F.R. Pavan, R. Sesti-Costa, T.A. Heinrich, C.M. Costa-Neto, 6-Mercaptopurine complexes with silver and gold ions: Anti-tuberculosis and anti-cancer activities, Biomed. Pharma. 65 (2011) 334.

[6] S.A. Silva, C.Q.F. Leite, F.R. Pavan, N. Masciocchi, A. Cuin, Coordinative versatility of a Schiff base containing thiophene: Synthesis, characterization and biological activity of zinc(II) and silver(I) complexes, Polyhedron 79 (2014) 170.

[7] I.L. Paiva, G.S.G. Carvalho, A.D. Silva, P.P. Corbi, F.R.G. Bergamini, A.L.B. Formiga, R. Diniz, W.R. Carmo, C.Q.F. Leite, F.R. Pavan, A. Cuin, Silver(I) complexes with symmetrical Schiff bases: Synthesis, structural characterization, DFT studies and antimycobacterial assays, Polyhedron 62 (2013) 104.

[8] M. Darawsheha, H.A. Alia, A.L. Abuhijleha, E. Rappocciolob, M. Akkawic, S. Jaberc, S. Maloula, Y. Husseinb, New mixed ligand zinc(II) complexes based on the antiepileptic drug sodium valproate and bioactive nitrogen-donor ligands. Synthesis, structure and biological properties, Eur. J. Med. Chem. 82 (2014) 152.

[9] H. Wang, H. Yuan, S. Li, Z. Li, M. Jiang, Synthesis, antimicrobial activity of Schiff base compounds of cinnamaldehyde and amino acids, Bioorg. Med. Chem. Lett. 26 (2016) 809.

[10] K. Karupaiyan, V.G. Puranik, A.R.A.S. Deshmukh, B.M. Bhawal, Stereoselective synthesis of cis-Bis-β-lactams linked with an ethylene bridge, Tetrahedron 56 (2000) 8555.

[11] A.A. Coelho, Indexing of powder diffraction patterns by iterative use of singular value decomposition, J. Appl. Crystallogr. 36 (2003) 86.

[12] TOPAS-R, General Profile and Structure Analysis Software for Powder Diffraction Data, Version 4.2, Karlsruhe, Germany, Bruker AXS, 2009.

[13] G.S. Pawley, Unit-cell refinement from powder diffraction scans, J. Appl. Crystallogr. 14 (1981) 357.

[14] A.L. Spek, Structure validation in chemical crystallography, Acta Crystallogr. D 65 (2009) 148.

[15] A. Coelho, Whole-profile structure solution from powder diffraction data using simulated annealing, J. Appl. Crystallogr. 22 (2000) 899.

[16] A.D. Khalaji, M. Weil, Crystal Structure of N, N′-Bis(trans-cinnamaldehyde) ethylenediimine, Anal. Sci. 23 (2007) 187.

[17] R.A. Young, The Rietveld Method, IUCr Monograph N.5, Oxford University Press, New York, 1981.

[18] J.C. Palomino, A. Martin, M. Camacho, H. Guerra, J. Swings, F. Portaels, Resazurin microtiter assay plate: simple and inexpensive method for detection of drug resistance in Mycobacterium tuberculosis, Antimicrob. Agents Chemother. 46 (2002) 2720.

[19] V.Z. Mota, G.S.G. de Carvalho, P.P. Corbi, F.R.G. Bergamini, A.L.B. Formiga, R. Diniz, M.C.R. Freitas, A.D. da Silva, A. Cuin, Crystal structure and theoretical studies of the keto-enol isomerism of N, N′-bis(salicylidene)-o-phenylenediamine (salophen), Spectrochim. Acta, Part A: Mol. Biomol. Spectrosc. 99 (2012) 110.

[20] J.H.B. Nunes, R.E.F. de Paiva, A. Cuin, W.R. Lustri, P.P. Corbi, Silver complexes with sulfathiazole and sulfamethoxazole: Synthesis, spectroscopic characterization, crystal structure and antibacterial assays, Polyhedron 85 (2015) 437.

[21] L.F. Marques, A. Cuin, G.S.G. De Carvalho, M.V. Dos Santos, S.J.L. Ribeiro, F.C. Machado, Energy transfer process in highly photoluminescent binuclear hydrocinnamate of europium, terbium and gadolinium containing 1,10-phenanthroline as ancillary ligand, Inorg. Chim. Acta 441 (2016) 67.

[22] S. Alvarez, D. Avnir, Continuous chirality measures of tetracoordinate bis (chelate) metal complexes, Dalton Trans. (2003) 562.